Chromospheric and coronal magnetic field measurements

Andreas Lagg

Max-Planck-Institut für Sonnensystemforschung, Katlenburg-Lindau

Measurement methods:

- in situ
- remote
  - radio measurements
  - loop oscillations
  - coronal Zeeman effect
  - Hanle / Zeeman diagnostics (chromosphere)

Some results:

- Canopy
- 3D structure of chromosphere
- uncombed chromopshere
- current sheets

- Helios 1+2, Mariner, Pioneer (Behannon 1978, Mariani et al. 1978 & 1979): measurements from >0.3 AU (= 64 R_S)

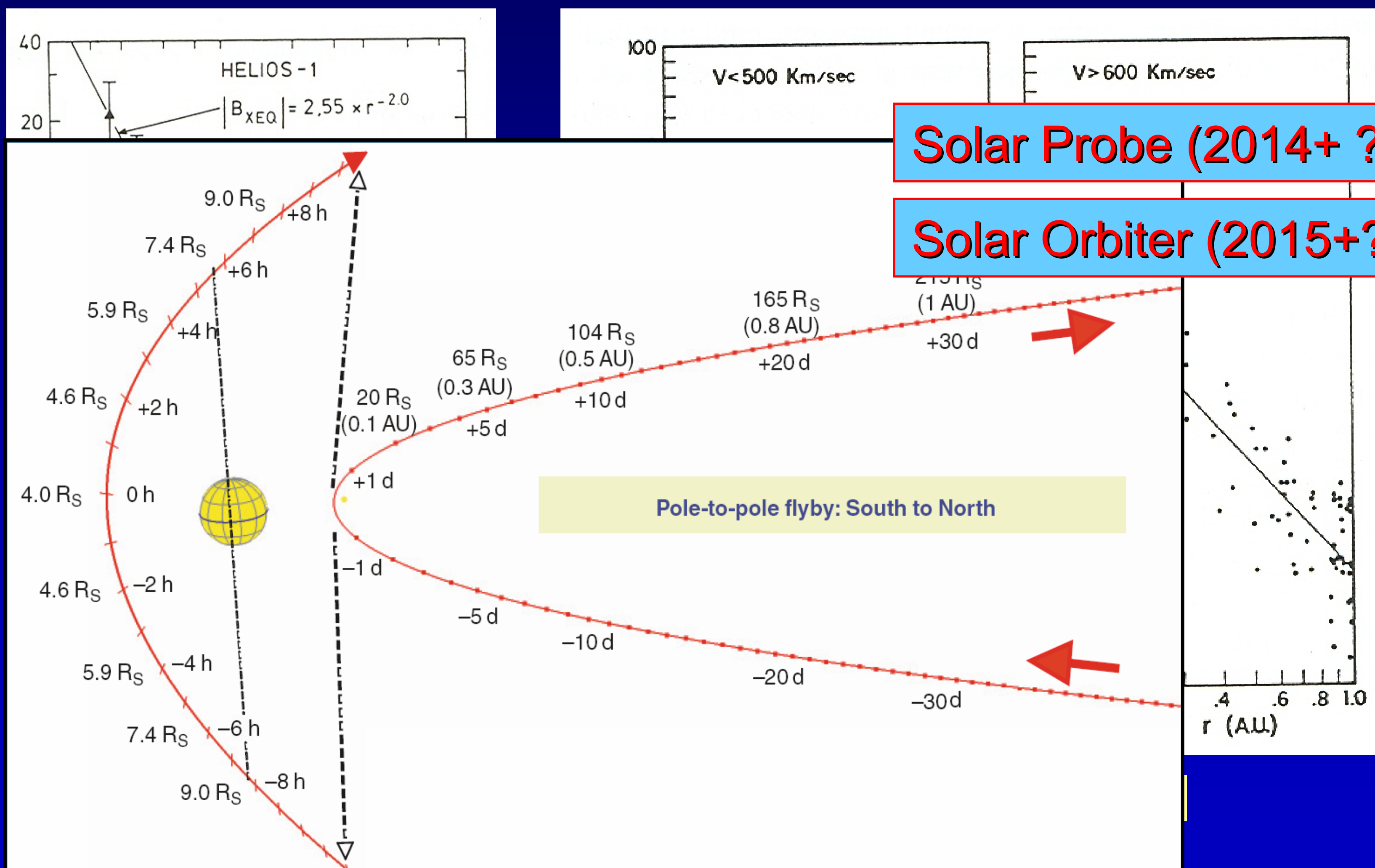

Solar Probe (2014+ ?): > 4 R_S

Solar Orbiter (2015+?): >40 R_S

properties of the radiation emitted or absorbed by magnetized plasma / gas:

- Bremsstrahlung emission
- coronal loop oscillations
- gyroresonant emission:
  radio observations of
  strong field regions (>250 G)
- Faraday rotation:
  radio observations
- Hanle effect:
  spectropolarimetric observations UV - IR
- Zeeman effect:
  spectropolarimetric observations (> IR)
- Resonance scattering (< UV)

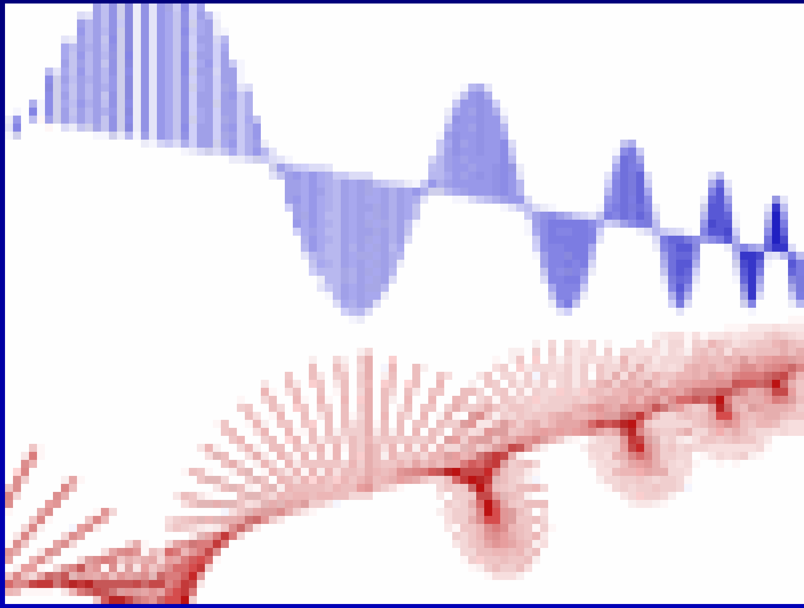

Polarisation!

- (Extrapolations, simulations)

difficulties

Corona:

- low magnetic field:
  ~10 G: $Q/I = 10^{-1}$, $V/I = 10^{-3}$-10^{-4}
- low emission
- large temporal variations
- LOS integration

Chromosphere:

- cancellation effects
- non-LTE
- complex line formation

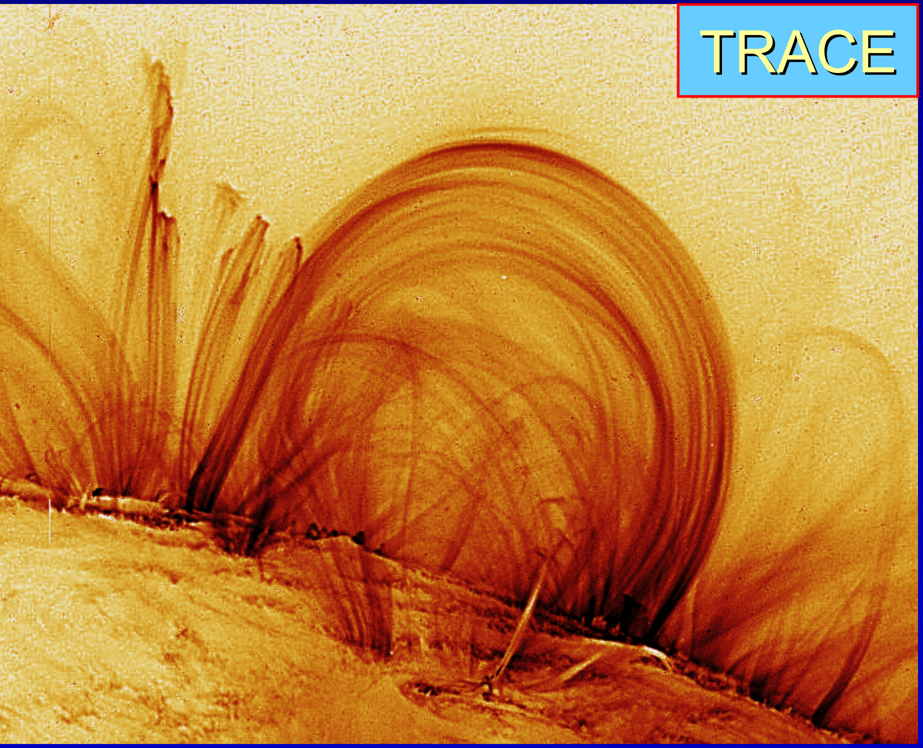

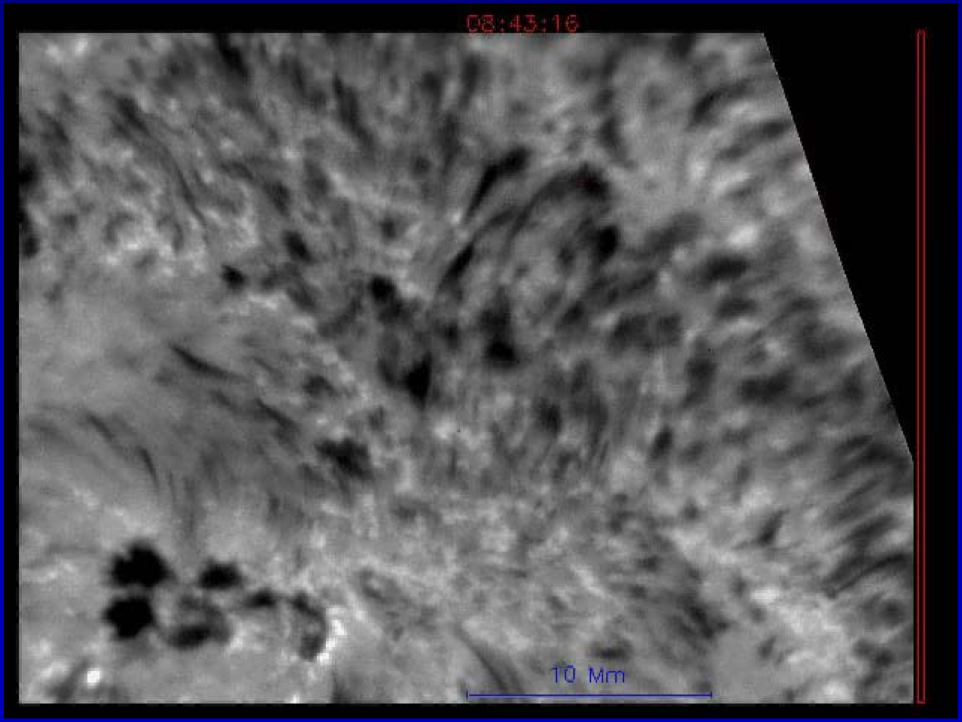

De Pontieu et al., 2004

Radio Measurements – Faraday Rotation

- plane of linear polarization is rotated by magnetized plasma with density n_e:

→ measures product of electron density and LOS-component of magnetic field

$$\Delta\chi \propto \int_{LOS} n_e \vec{B} \cdot d\vec{s}$$

[Nicholson 1983]

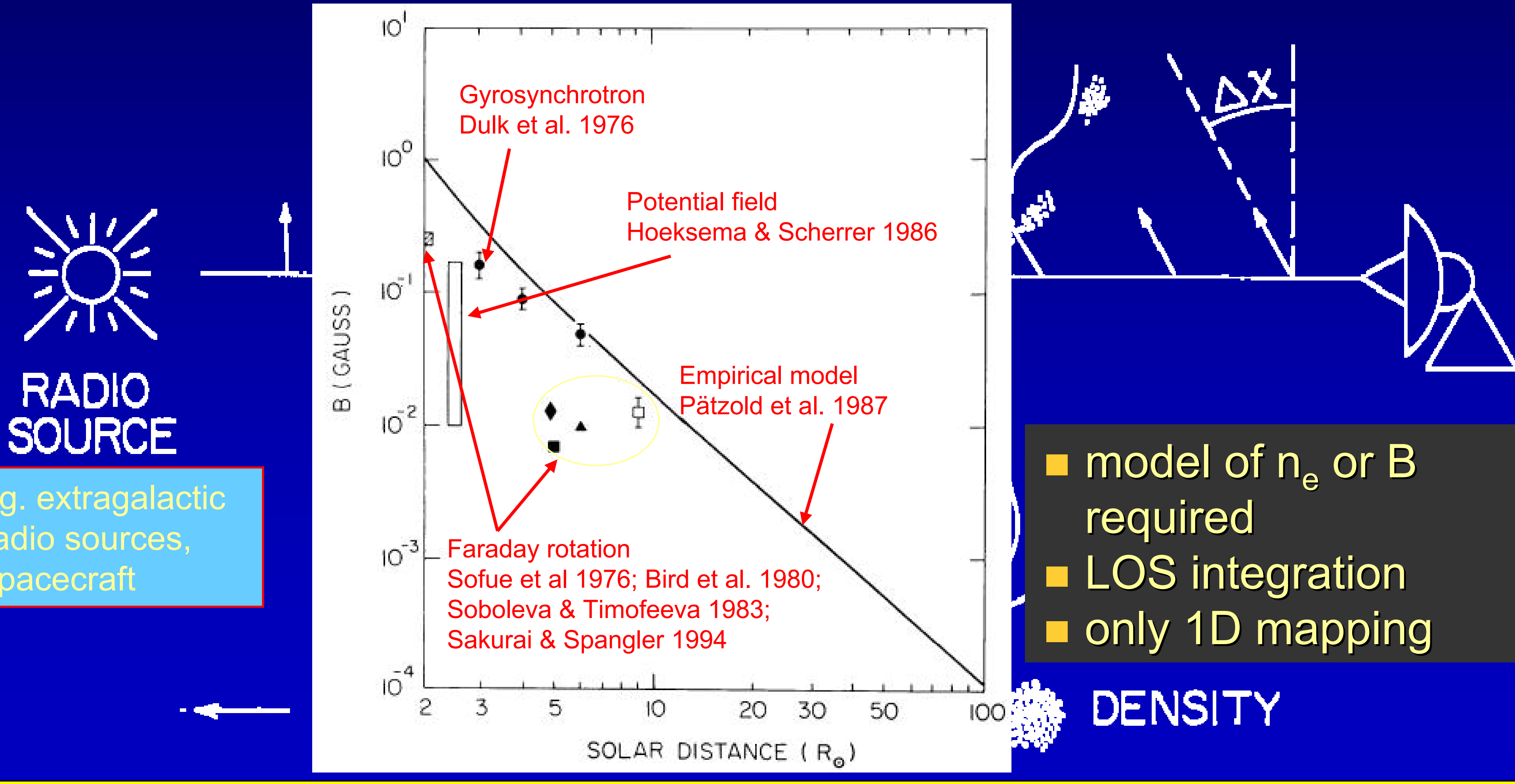

eg. extragalactic radio sources, spacecraft

- model of n_e or B required
- LOS integration
- only 1D mapping

Radio Measurements

- Bremsstrahlung:
  results from collisions of e^- with ions
  ➔ electron density diagnostic tool
- Gyroresonance:
  emission from nonrelativistic thermal plasma at low harmonics of the electron gyrofrequency, $f_B = 2.8\,B$ MHz
- Gyrosynchrotron:
  emission by mildly relativistic electrons at harmonics 10-100 of the gyrofrequency
- Plasma emission caused by electrostatic Langmuir waves

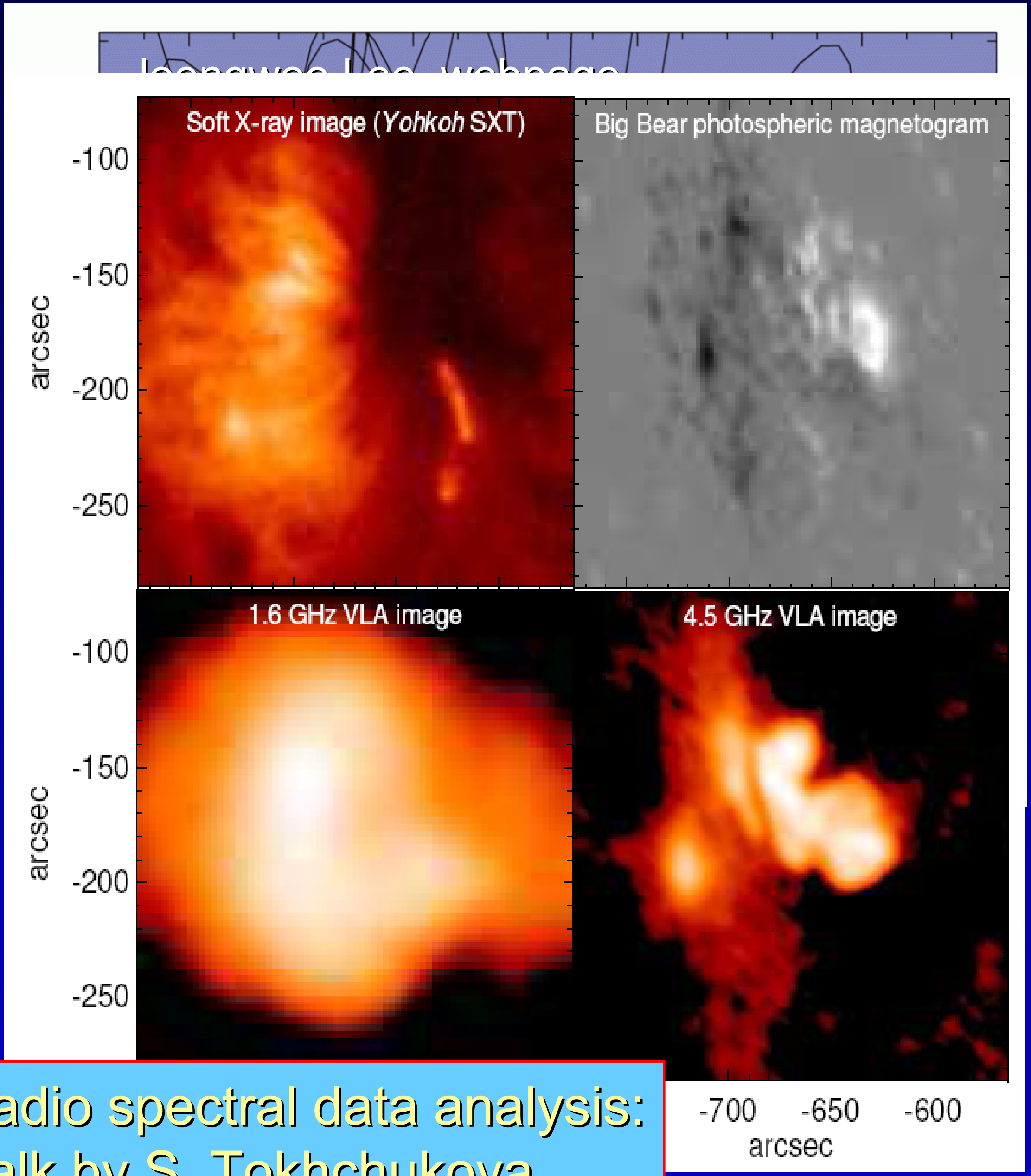

radio spectral data analysis:
talk by S. Tokhchukova

[White 2002]

Loop Oscillations

phase speed $C_p = 2L/P$, $C_{Ain} < C_p < C_{Aout}$
kariakov, 2004]

phase speed = v_A
observable: period

long. density fluctuation (C_S),
weak correlation to B

width

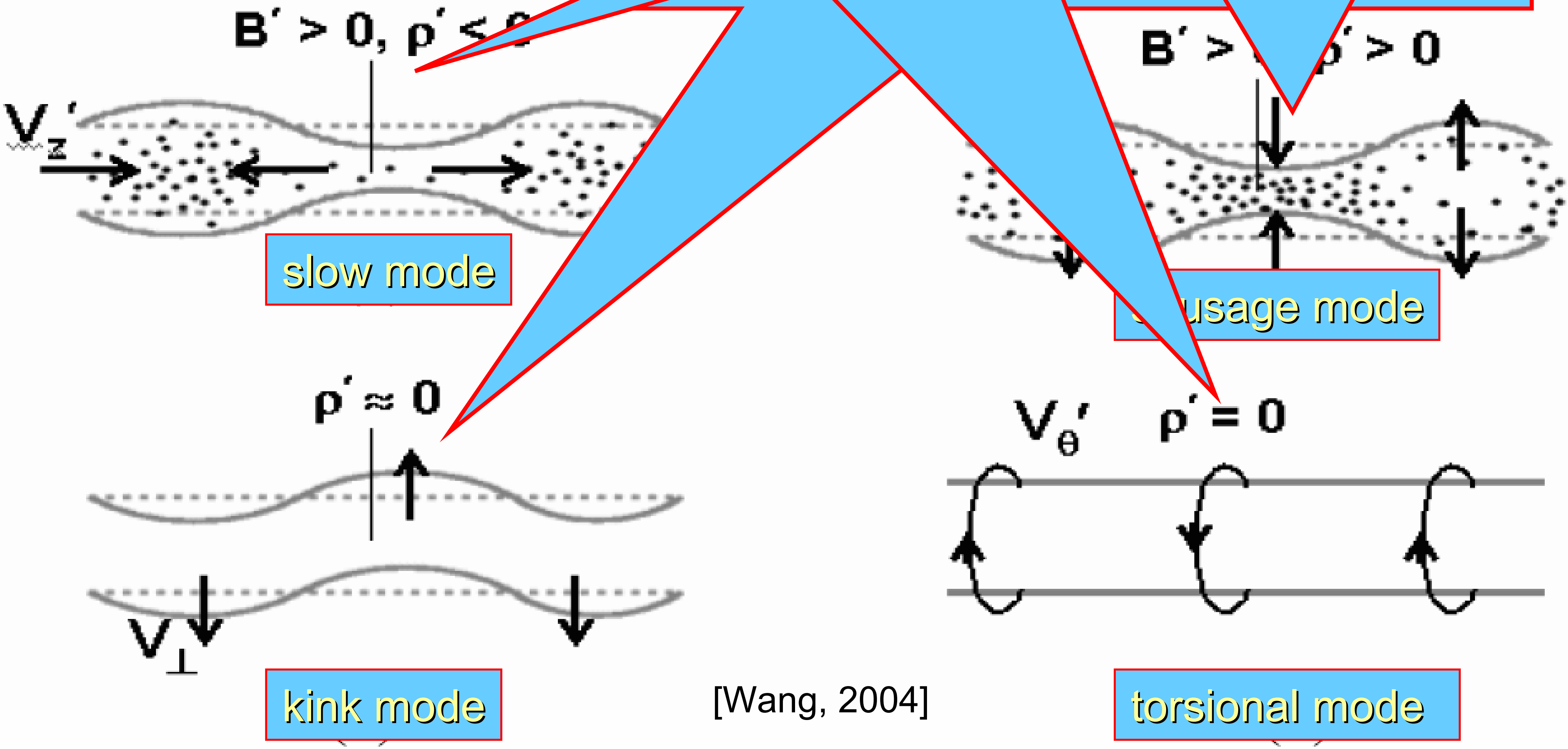

[Wang, 2004]

Loop Oscillations – results of magnetic field measurements

- Roberts et al. (1984)
  B = 15 G (observations: Koutchmy, 1983, fast kink wave)
- Nakariakov et al (2001): TRACE loop oscillations interpreted as global standing kink mode:
  → B = 13±9 G
- Asai (2001): periodic e^- acceleration in flare (P=6.6 s)
  kink mode → B = 400 G
  sausage mode → B = 120 G
  (Verwichte et al., 2005)

[Nakariakov et al. 2001]

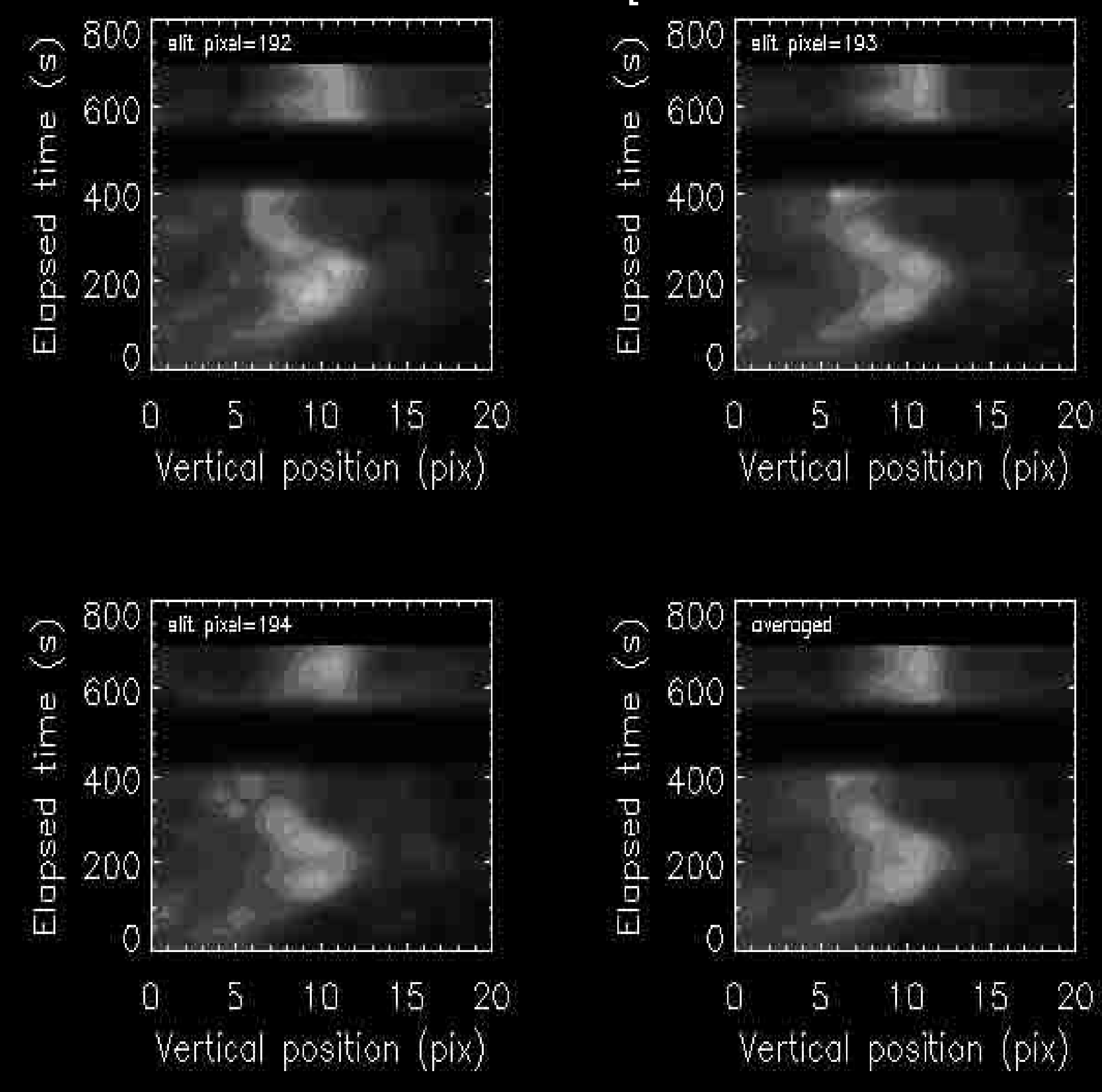

Loop Oscillations – results of magnetic field measurements

- Roberts et al. (1984)
  B = 15 G (observations: Koutchmy, 1983, fast kink wave)
- Nakariakov et al (2001): TRACE loop oscillations interpreted as global standing kink mode:
  → B = 13±9 G
- Asai (2001): periodic e⁻ acceleration in flare (P=6.6 s)
  kink mode → B = 400 G
  sausage mode → B = 120 G
  (Verwichte et al., 2005)

Asai et al. 2001

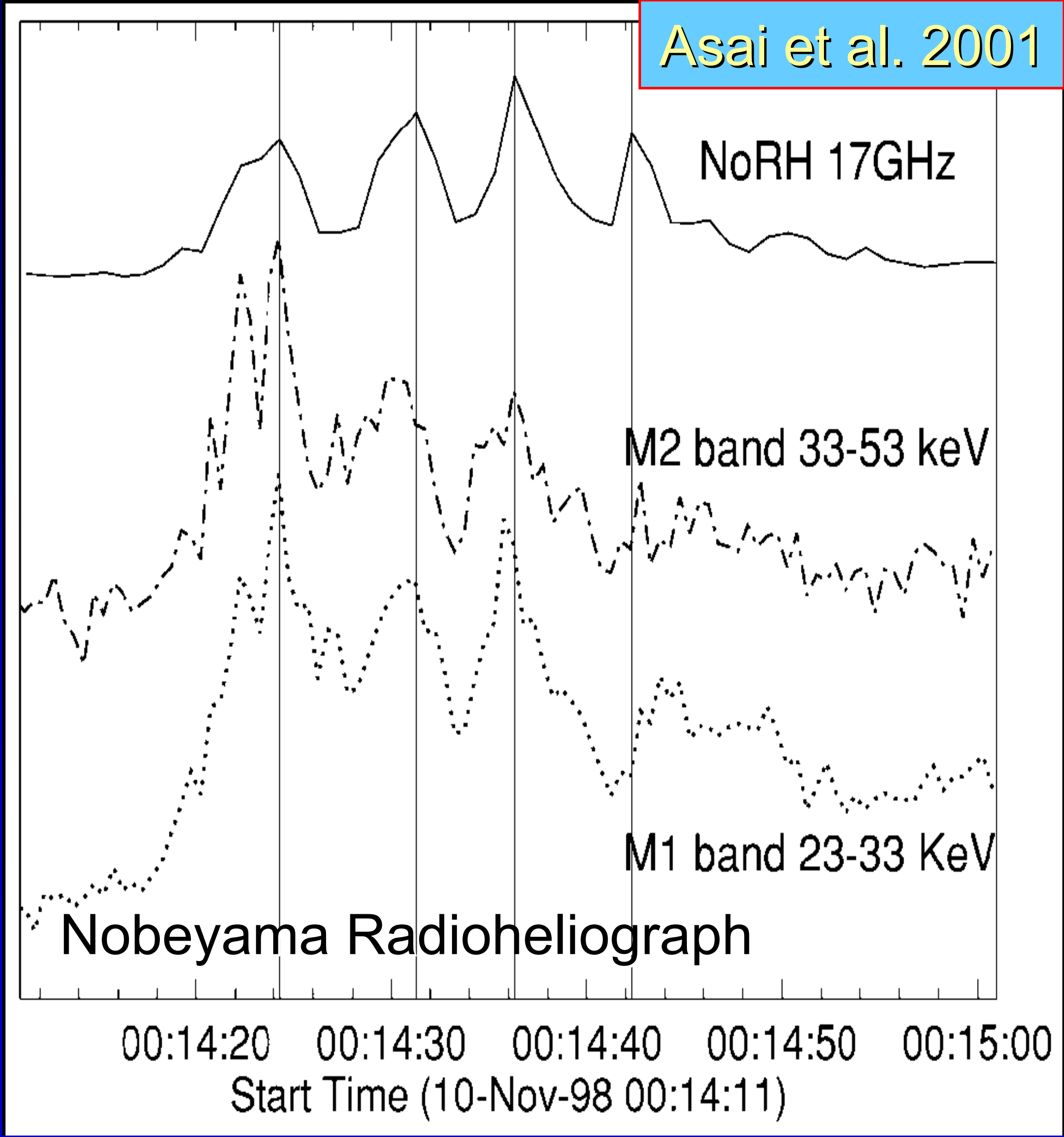

Coronal Zeeman effect

Problems:

- low B
- low emission
- LOS cancellation

IR (eg. Fe XIII 10747 Å, He 10830 Å) high sensitivity (10^{-4} and better)

first attempt: Harvey 1969
Fe XIV 5303 Å above active regions and in prominences:
$B = 13 \pm 20$ G

IR spectropolarimetry in Fe XIII 10747 Å:

- Kuhn (1995): B ≤ 40 G above active regions
- Lin (2000): $B(1.12 - 1.15\ R_\odot) = 10 – 33$ G

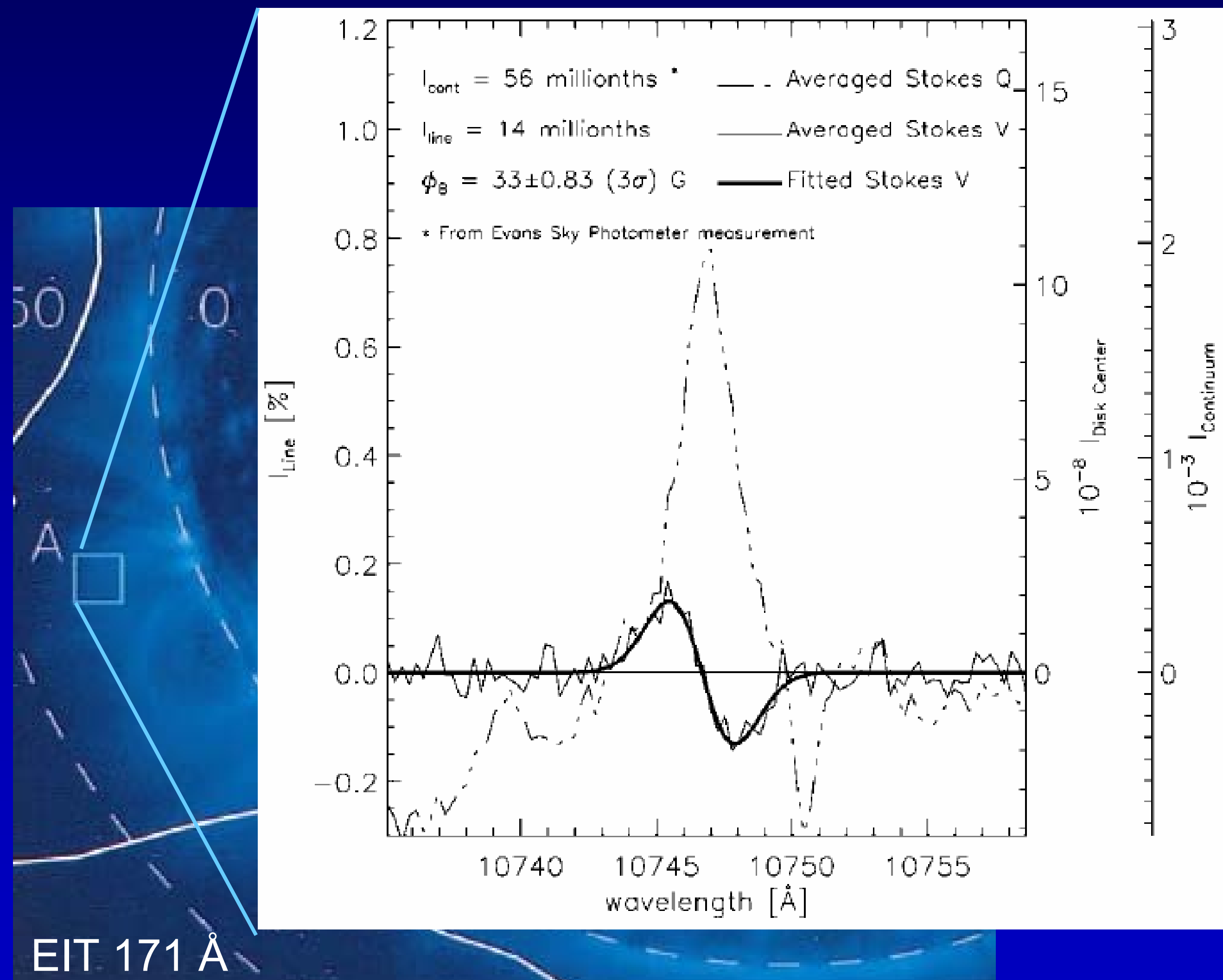

Coronal Zeeman effect – 2D

Lin et al. (2004): SOLARC/OFIS

- first 2D measurement using Fe XIII Zeeman polarimetry
- flux density: 4 G

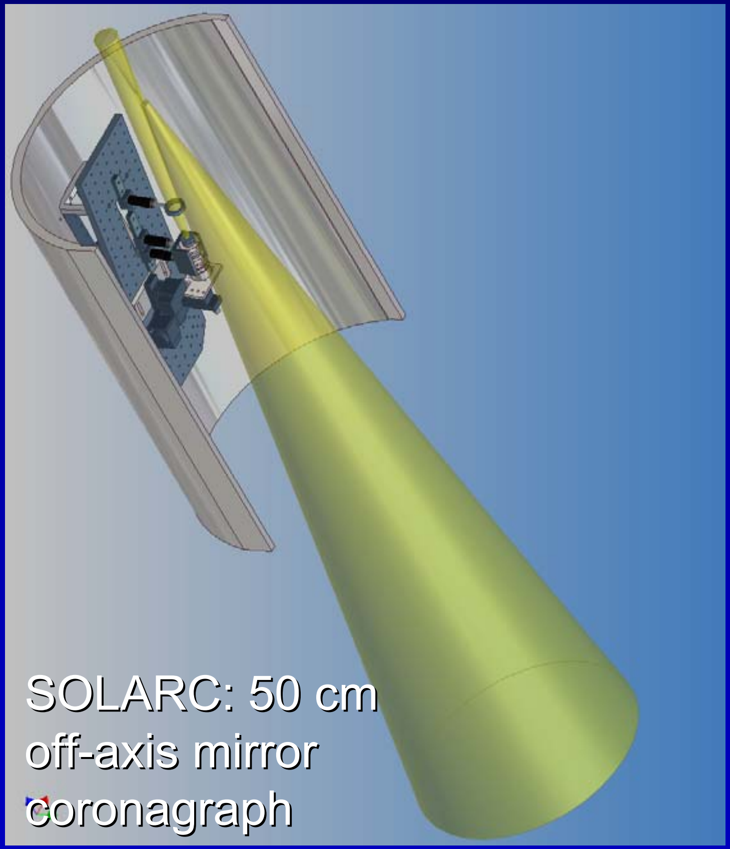

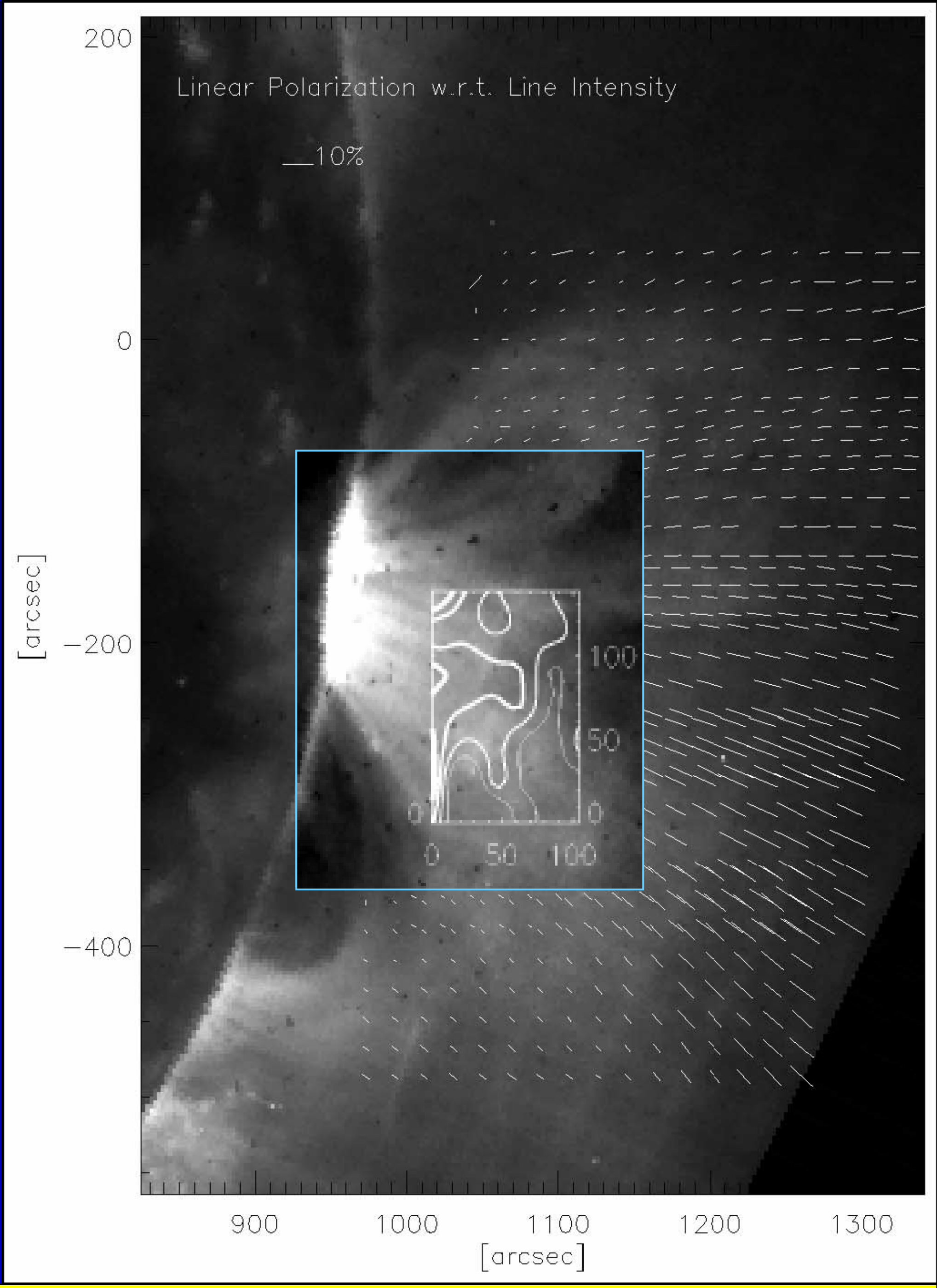

Coronal Zeeman effect – 2D

Coronal Multi-channel Polarimeter: (CoMP): IQUV from

- Fe XIII 1074.4, 1079.8 (coronal)
- He I 1083.0 (prominences)

ATST:
expect measurments in the sub-Gauss range

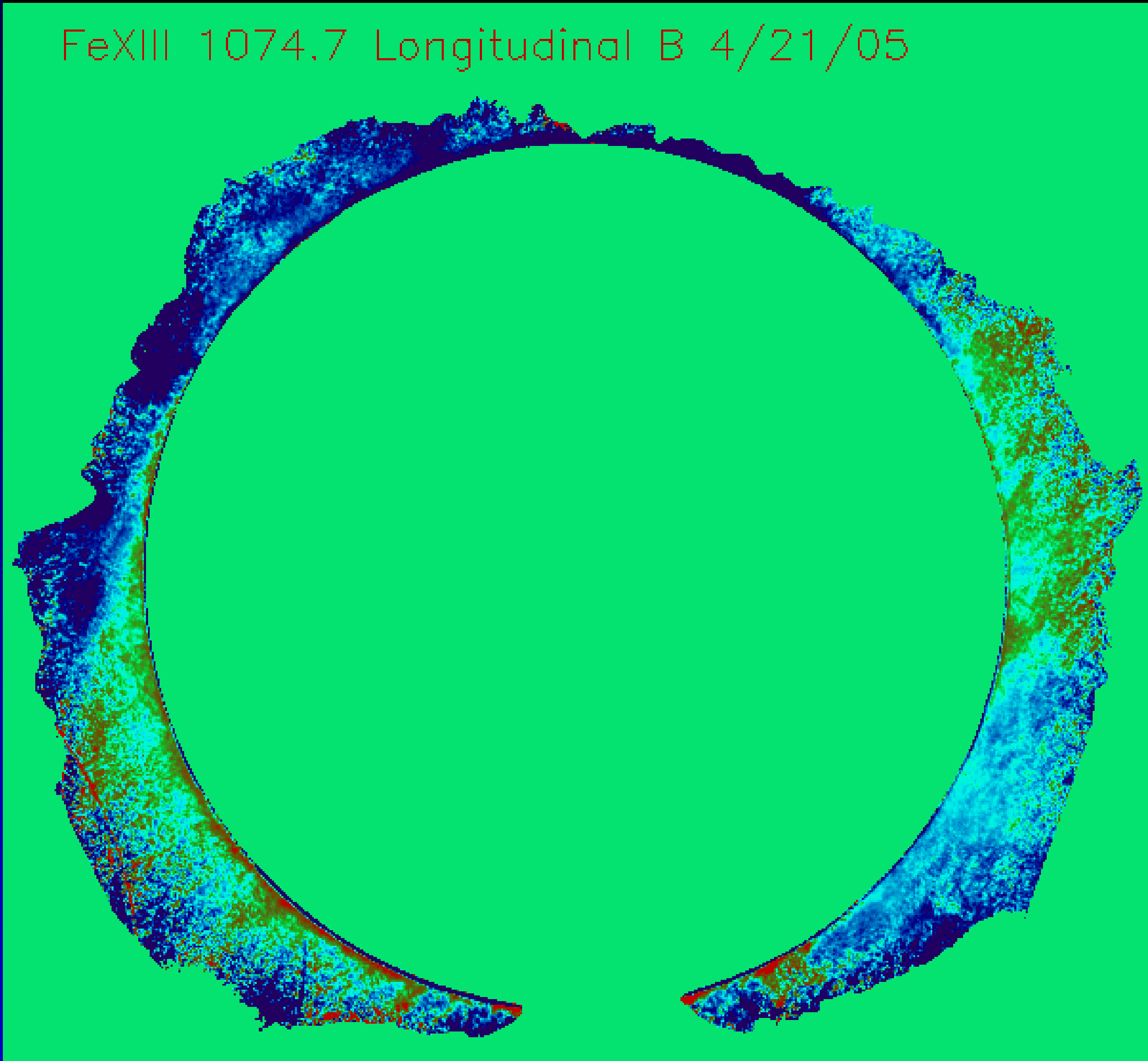

S. Tomczyk, 2004

Hanle-Effect

Trujillo-Bueno (2002)

magnetic case:
now the 3 oscillators are not independent:

- 1 osc. along B (ω0)
- 2 osc. around B ($\omega_0-\omega_L$; $\omega_0+\omega_L$)
- damped oscillation precesses around B
  → rosette like pattern
  → damping time tlife = 1/γ

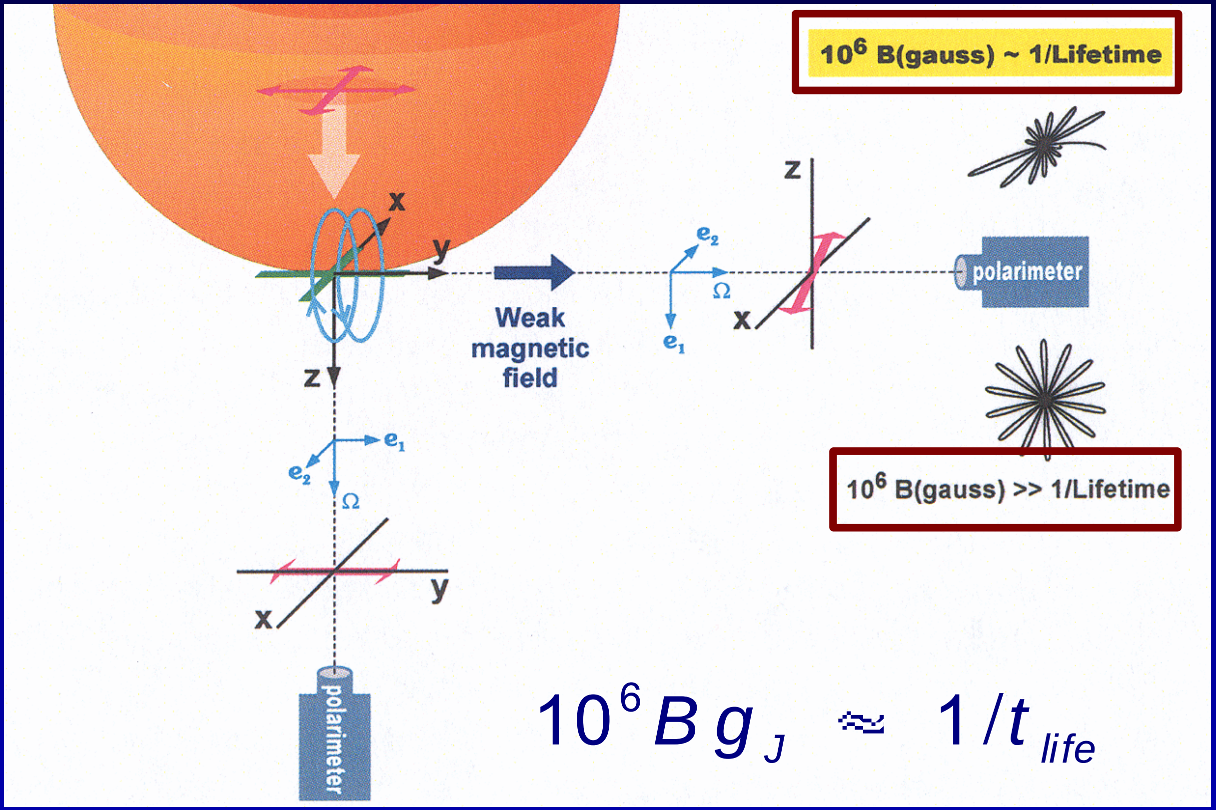

- $\omega_B \gg 1/t_{life}$
  - forward scattering: max. polarization along ±y
  - 90° scattering: no polarization
- $\omega_B \approx 1/t_{life}$
  - forward scattering: weaker, but still ±y
  - 90° scattering: lin.pol. in Q, U, smaller than in non-magnetic case

He 1083: atomic polarization

Magnetic field in spicules

- Hanle / Zeeman diagnostics of spicule in He 1083 nm multiplet
- 1st direct empirical demonstration of magnetized, spicular material
- magnetic field parameters (2000 km):
  - B = 10 G
  - Θ = 35° (to local vertical)
  - $v_{Thermal}$ = 22 km/s

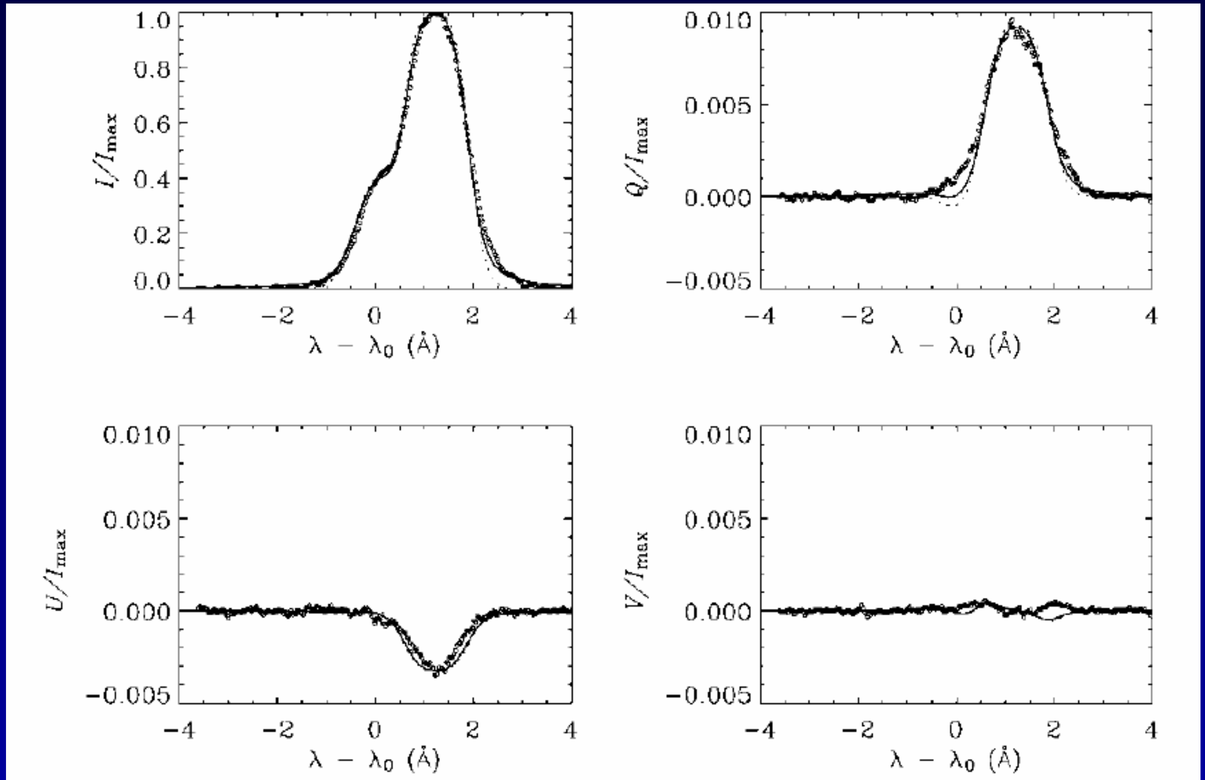

FIG. 2.—*Open circles*: Observed Stokes profiles at the same spatial point of Fig. 1. The reference direction for Stokes Q is the parallel to the solar limb. The origin of the wavelength scale corresponds to the blue component of the He I λ10830 multiplet. *Dotted line*: Optically thick theoretical modeling ($\tau_{red} = 3.7$) for a magnetic field strength $B = 10$ G, inclination $\theta_B = 37°$, azimuth $\chi_B = 173°$, and a thermal velocity of 15 km s^{-1}. *Solid line*: Optically thick theoretical modeling ($\tau_{red} = 3$) with enhanced damping parameter, for a magnetic field strength $B = 10$ G, inclination $\theta_B = 37°$, azimuth $\chi_B = 173°$, and a thermal velocity of 13.5 km s^{-1}. In both modeling cases, the alternative determination $B = 10$ G, $\theta'_B = 180° - \theta_B$, and $\chi'_B = -\chi_B$ gives the same theoretical Stokes profiles.

Trujillo Bueno et al., 2005

also: Lopez Ariste (2005)

Chromospheric magnetic structures

He 10830 Zeeman / Hanle diagnostics

- Paschen-Back implementation
- robust inversion technique
- Milne-Eddington based
- TIP / TIP2 data (VTT)

Apply to:

- Canopy
- downflows in small scale fibrils

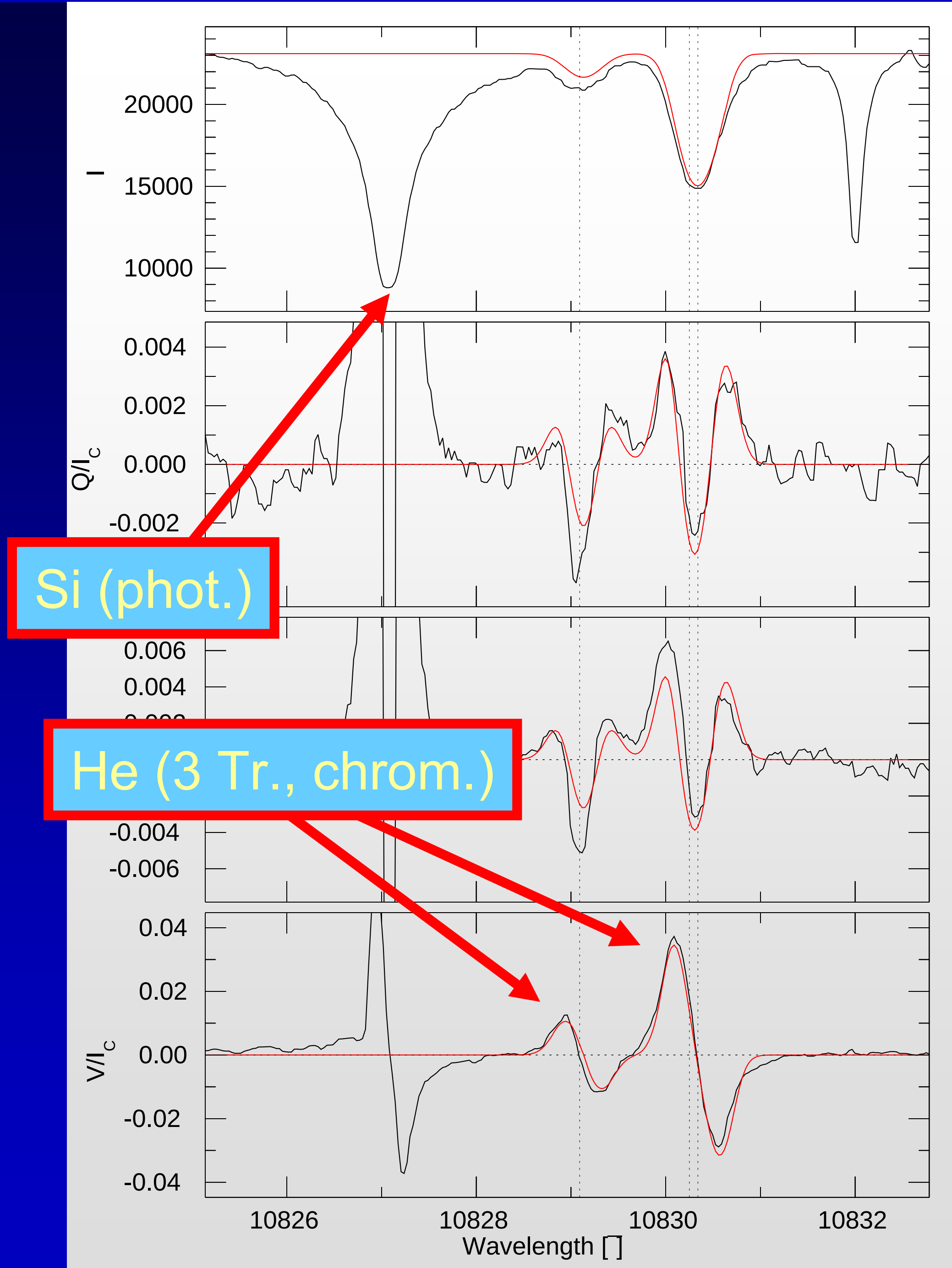

./ps/zeeman.eps

Magnetic Canopy

(Gabriel, 1976)

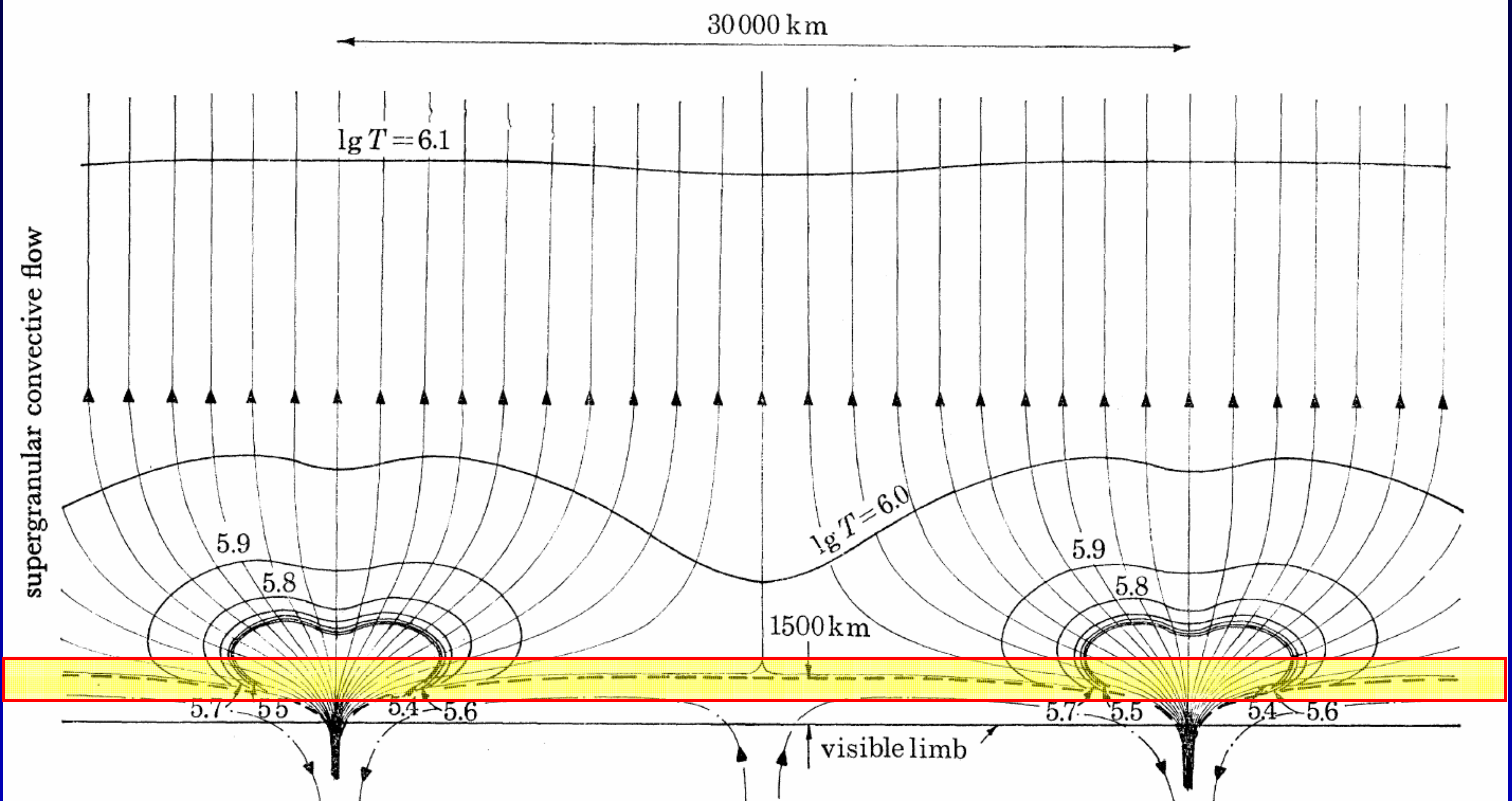

FIGURE 5. The proposed structure of the network model based upon energy balance (model C), showing the convection cell, magnetic field lines and contours of constant temperature. The primary transition region is indicated by the converging contours of temperature. The secondary transition region is shown by the dashed line.

Giovanelli (1980), Solanki & Steiner (1990): lower canopy height (600-1200 km)

Theoretical Aspects of Canopy Fields

- relatively strong internetwork fields (few Mx/cm^2) destroy classical canopy (wineglass shape)
  ➔ 50% of coronal field rooted in internetwork
- canopy field lines return to photosphere near parent flux tube
- Sanchez-Almeida et al. (2004): bright points in internetwork tracing magnetic field concentrations

Schrijver & Title (2003)

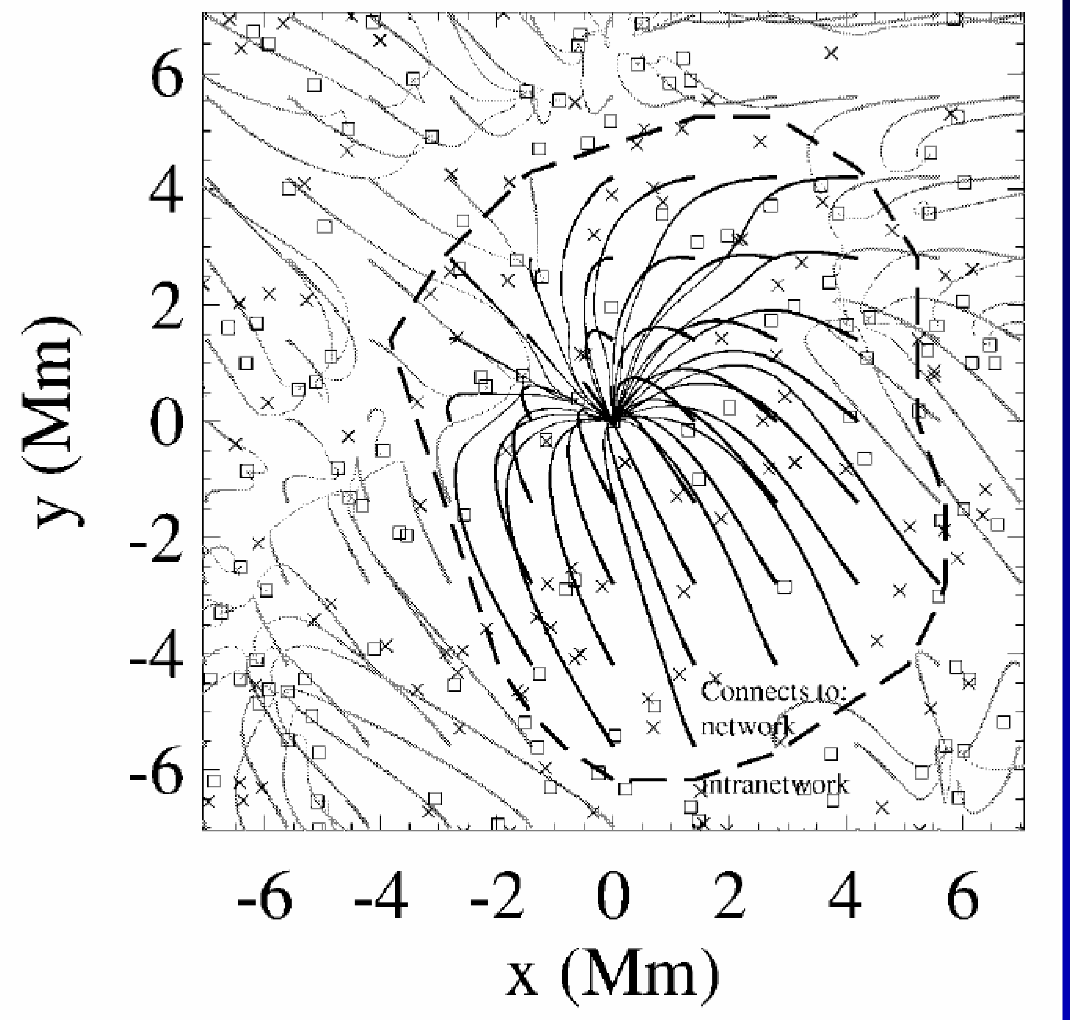

FIG. 4.—Similar to Fig. 1 but showing the field lines starting from a grid 7 Mm above the source plane. Field lines terminating on the central network source are black and on the internetwork sources gray. The dashed curve encloses the flux from the network source that reaches up to greater than 7 Mm; without internetwork field that perimeter would equal the field of view, thus forming the classical network canopy that covers the entire photosphere.

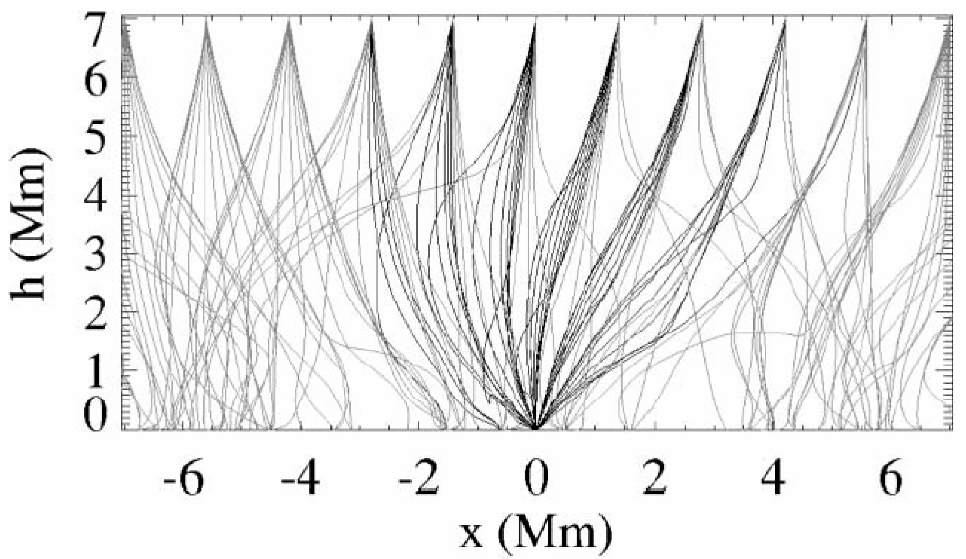

Canopy measurement He 10830

- TIP2: Si 10827 & He 10830
- quiet sun + network field, Θ=60°
- RMS noise 5E-4

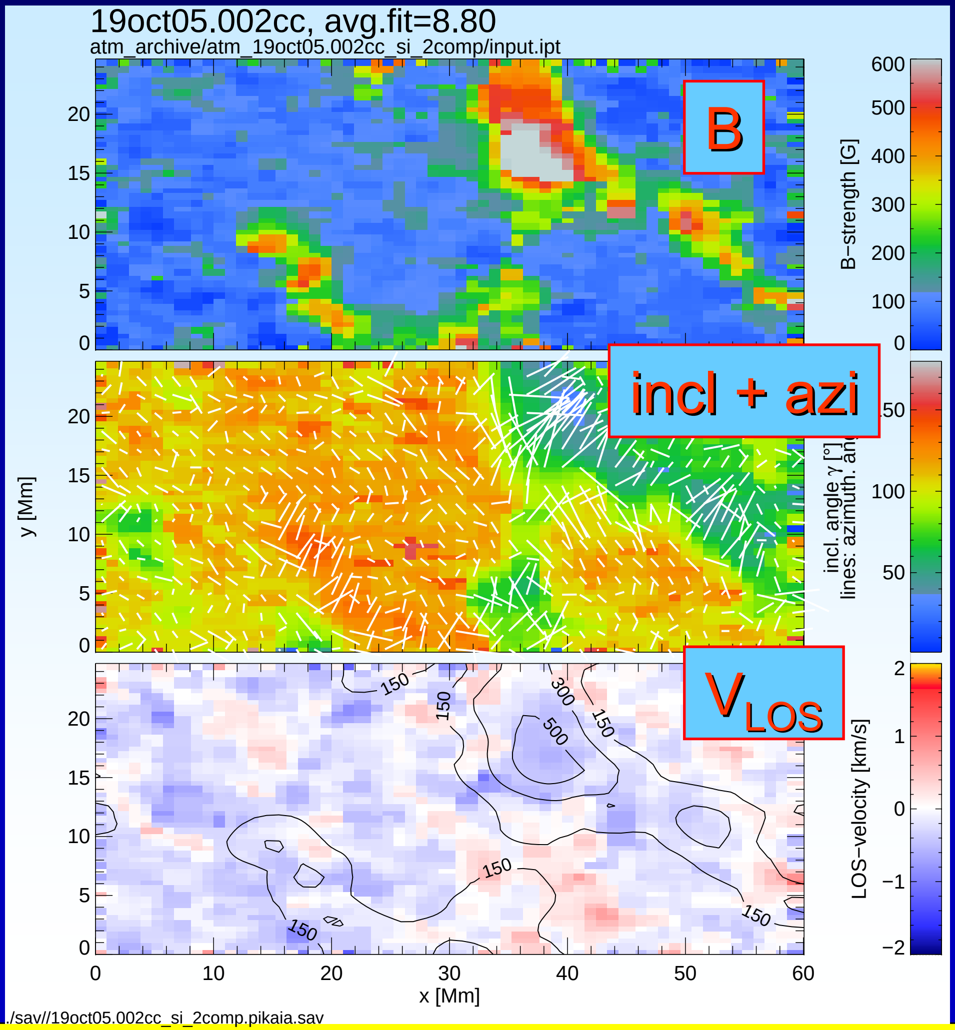

Photosphere (Si 10827)

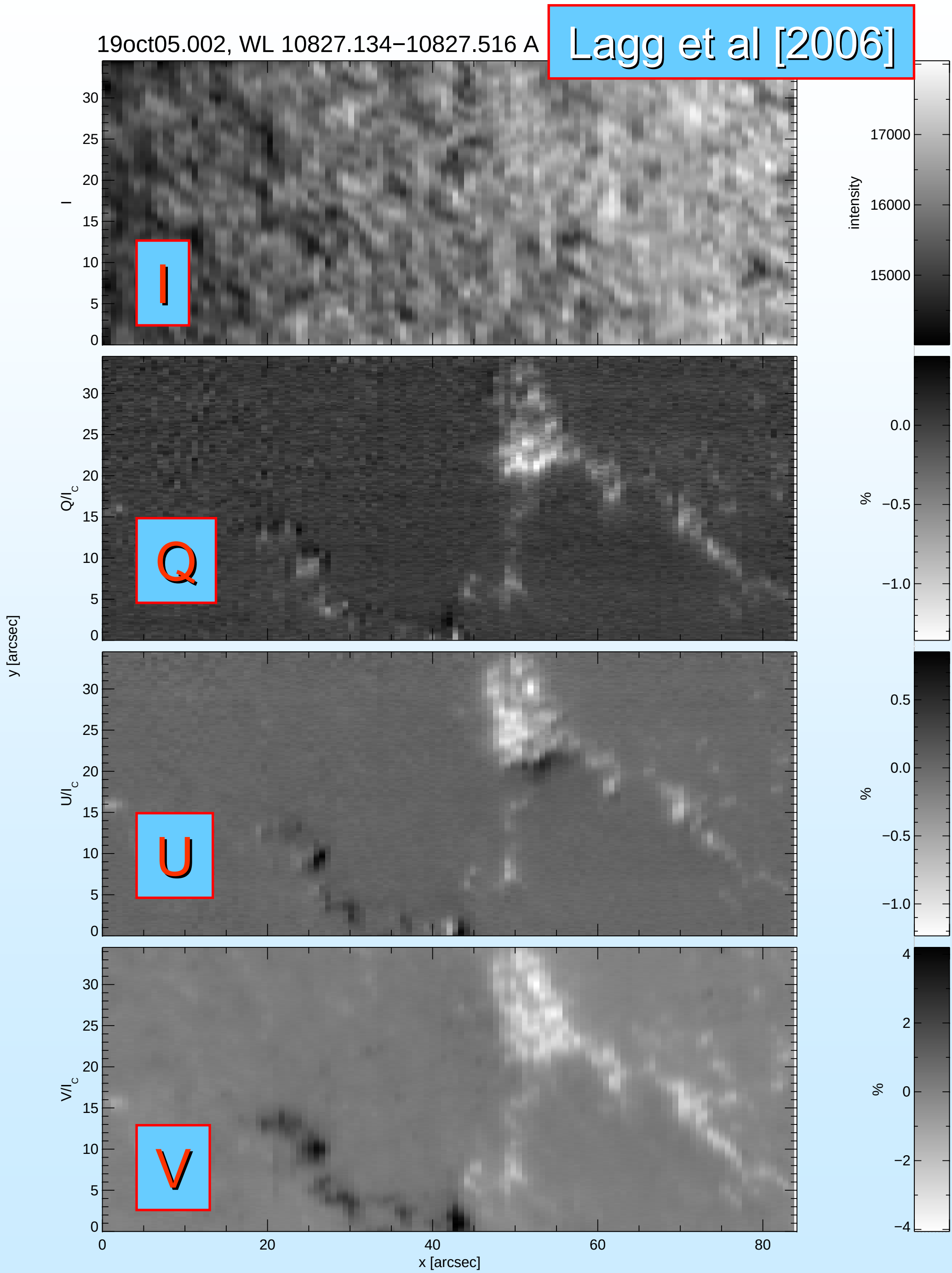

Canopy measurement He 10830

Chromosphere (He 10830)

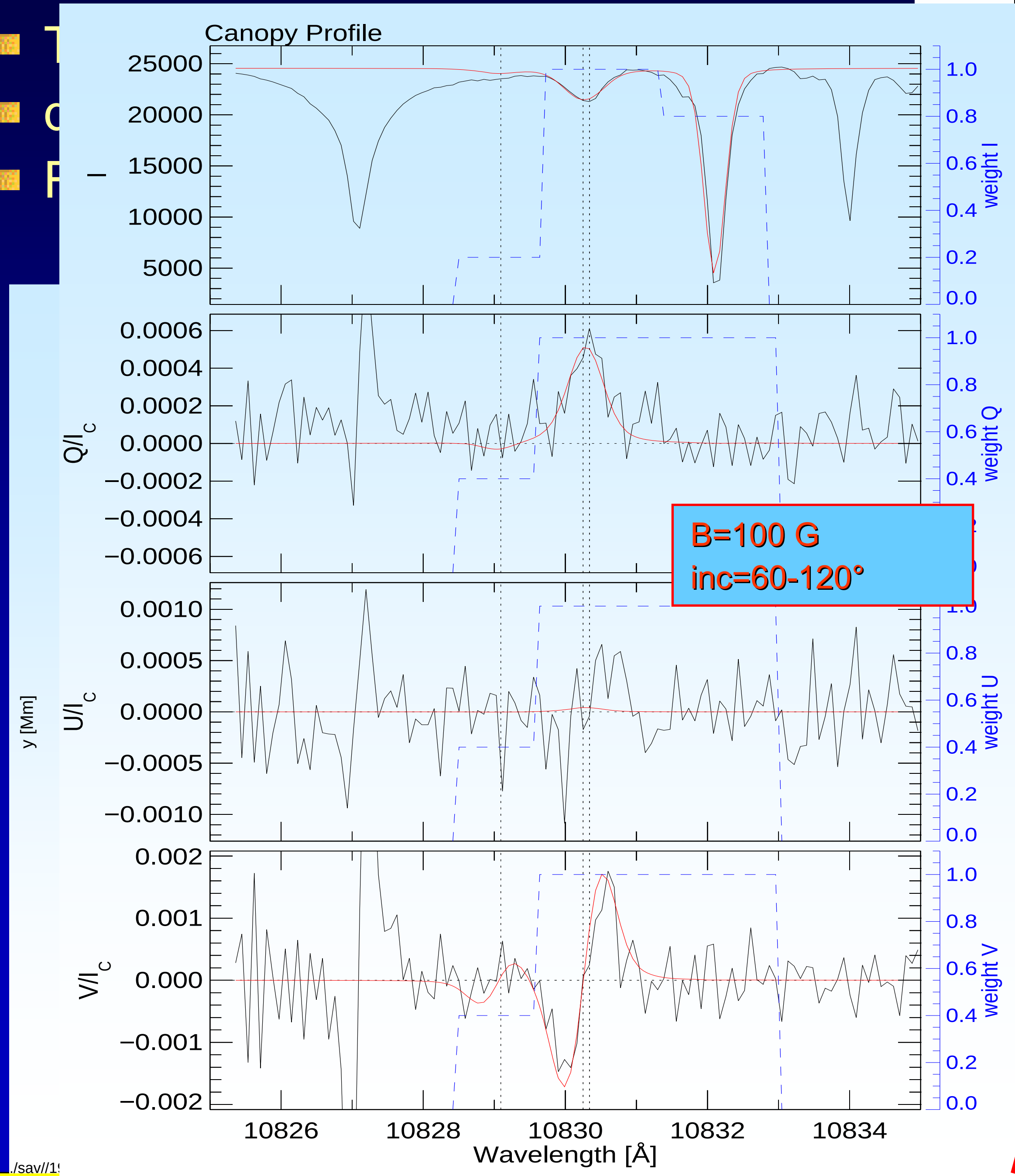

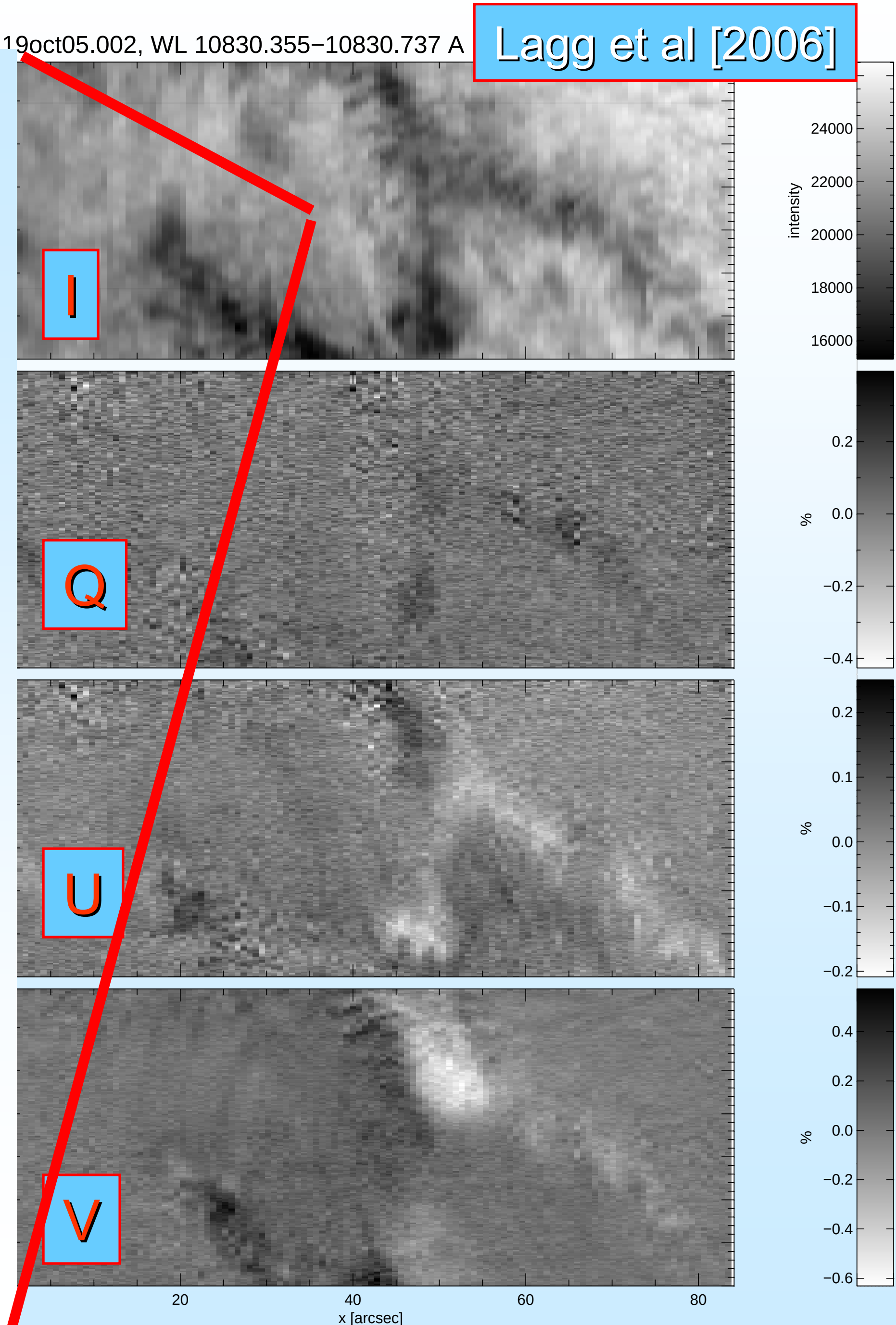

Example: multi component Downflows

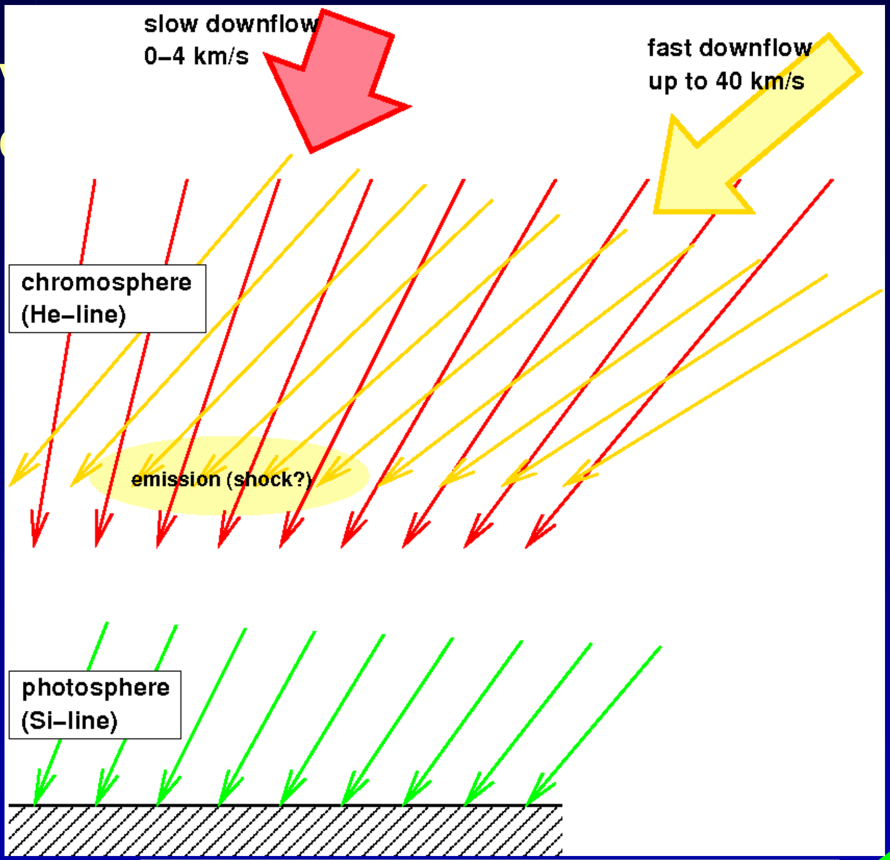

Slow Component:			
VLOS	B	Incl.	Azim
-620 m/s	520 G	33°	-14°

Fast Component:			
VLOS	B	Incl.	Azim.
24900 m/s	730 G	67°	10°

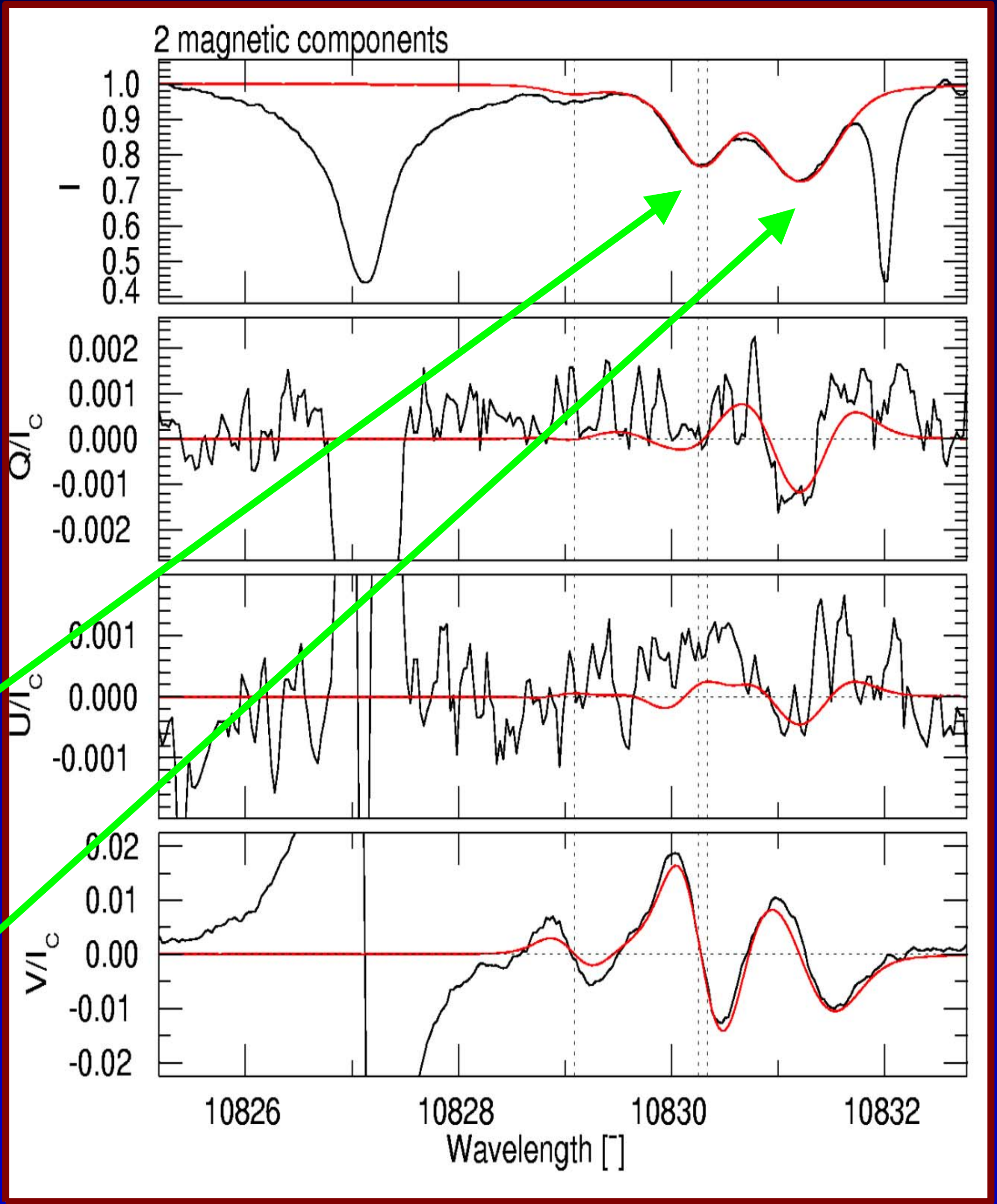

Downflows: multi-component

Supersonic downflows are very common

- Every region has locations with 2-4 magnetic components in 1 pixel.
- 1 comp nearly at rest, the others exhibit strongly supersonic downflows (Mach 3 & 6 in Fig.).
- Presence of unresolved fine structure (field may show different inclinations for different velocity components)

Sasso [2006]

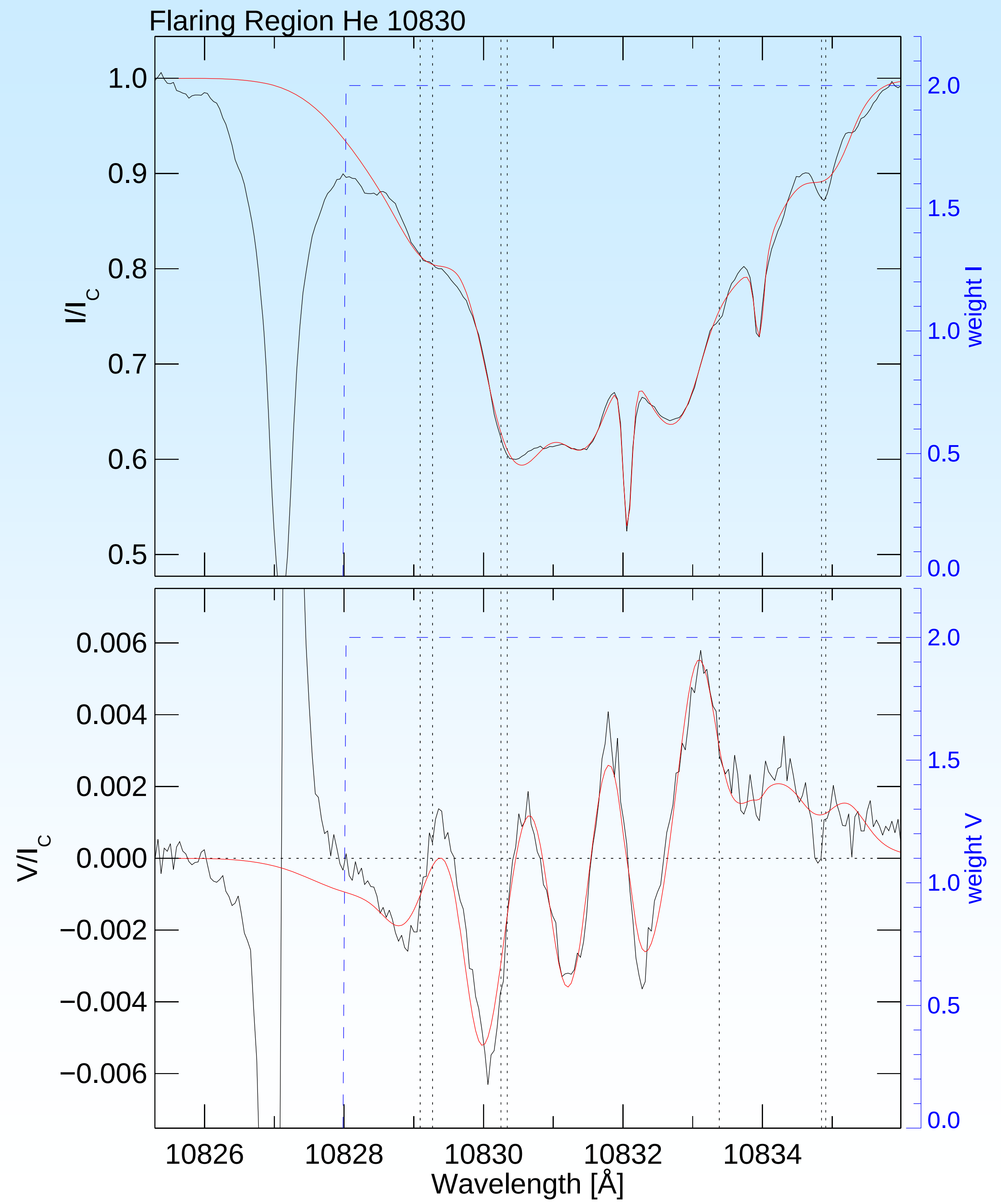

Outlook

- aera of reliable chromospheric & coronal magnetic field measurements has just started
- promising advances
  - observational techniques
  - instrumentation
  - analysis techniques (inversions, extrapolations)
  - theoretical modelling
  - atomic physics
- the best is yet to come ...

Thank you!